JCTC Journal of Chemical Theory and Computation

Article

pubs.acs.org/JCTC

Time-Dependent Approach to Resonance Raman Spectra Including Duschinsky Rotation and Herzberg–Teller Effects: Formalism and Its Realistic Applications

Huili Ma,[†] Jie Liu,[†] and WanZhen Liang[‡,*]

[†]Hefei National Laboratory for Physical Science at Microscale, and Department of Chemical Physics, University of Science and Technology of China, Hefei 230026, People's Republic of China

[‡]Department of Chemistry, Xiamen University, Xiamen 361005, People's Republic of China

Supporting Information

ABSTRACT: Efficient quantum dynamical and electronic structure approaches are presented to calculate resonance Raman spectroscopy (RRS) with inclusion of Herzberg–Teller (HT) contribution and mode-mixing (Duschinsky) effect. In the dynamical method, an analytical expression for RRS in the time domain is proposed to avoid summation over the large number of intermediate vibrational states. In the electronic structure calculations, the analytic energy-derivative approaches for the excited states within the time-dependent density functional theory (TDDFT), developed by us, are adopted to overcome the computational bottleneck of excited-state gradient and Hessian calculations. In addition, an analytic calculation to the geometrical derivatives of the transition dipole moment, entering the HT term, is also adopted. The proposed approaches are implemented to calculate RR spectra of a few of conjugated systems, phenoxyl radical, 2-thiopyridone in water solution, and free-base porphyrin. The calculated RR spectra show the evident HT effect in those π-conjugated systems, and their relative intensities are consistent with experimental measurements.

1. INTRODUCTION

Due to its high sensitivity, RRS has become an important tool in analytical chemistry. It can reveal not only the molecular structure information, such as vibrational modes and mode-specific electron–phonon coupling, but also the molecular excited-state dynamics.[1−4] Theoretical prediction of RRS thus needs to combine the both electronic structure theories and quantum dynamical approaches to obtain the structure parameters and describe dynamics, respectively.[1,2,5−8]

The theoretical calculation of RRS starts from the well-known Kramers–Heisenberg–Dirac (KHD) polarizability tensor in the frequency domain. The straightforward methods are thus based on the eigenstate representation of the molecular vibrational modes, such as the sum-overstate (SOS) method.[9−14] The SOS method requires an explicit knowledge of all vibronic states contributing to the resonance effect. It is a most tedious calculation to sum all of the eigenstates of the vibrational modes in the molecular excited state, although several efficient techniques have been proposed.[9−14] As an alternative, Green's function technique has been introduced to transform the KHD formula to the time domain, where the tedious SOS calculation is replaced by the propagation of a wavepacket on the excited-state surface. On the basis of this idea, Lee and Heller have proposed the time-dependent approach to RRS.[15−17] Since then, the time-dependent approach has been broadly applied to predict and explain experimental measurements (for instance, see ref 2, and references therein).

In the conventional time-dependent approaches, it is assumed that the mode frequencies on the molecular ground and excited states are the same, and the vibrational directions of modes on the two states are also the same, i.e., without the mode-mixing or Duschinsky rotation.[18] In this case, the propagation of the mode motions can be solved analytically under the Franck–Condon (FC) approximation (the transition dipole moment is a constant). The RRS under these approximations has been successfully used to measure mode-specific reorganization energies.[1] However, for many systems, especially the conjugated molecules, the vibrational frequencies and directions of the normal modes on the ground and excited states are different. Several theoretical works[16,19−21] indeed have shown that the Duschinsky rotation significantly affects the RRS intensity. The time-dependent formalism to RRS with the inclusion of Duschinsky rotation has thus been derived by Heller and Tannor.[16,17] However, in that derivation, the FC approximation was assumed, which may be questionable for molecules with weakly allowed electronic transitions.

In the present paper, we theoretically investigate the RRS, including both the Duschinsky and non-Condon effects in the time domain. The non-Condon effect comes from the mode-coordinate dependence of the transition dipole moment. As the dipole moment is perturbationally expanded in terms of the mode coordinates, the contribution of the first term related to the linear coordinates is commonly called Herzberg–Teller (HT) effect.[24,25] The HT effect is generally much smaller than the FC contribution. However, it may significantly affect the RRS intensities for the molecules with the dipole-forbidden or weakly allowed transition states, in which the FC term becomes nearly zero. Indeed, several works[26,27] in the frequency domain have revealed the importance of both the Duschinsky and HT effects on RRS. One purpose of this paper is to present a time-dependent

Received: July 24, 2012
Published: September 20, 2012

approach, parallel to the methods in the frequency domain, to incorporate both effects on RRS. Moreover, the proposed approach may be straightforwardly applied to the higher-order HT terms with a slightly more computational cost. Quite recently, we note that the time-dependent formalism to RRS has already been derived to include the HT effect,[22,23] in which the Duschinsky rotation is ignored.

To theoretical yield RRS of concrete molecules, the remaining problem is to evaluate the electronic structure parameters for molecular properties, such as the equilibrium structures, the vibrational frequencies, normal modes of both ground and excited states, and the excitation energies, transition dipole moments and their geometrical derivatives as well. Nevertheless, the calculations on these physical quantities are computationally more demanding and can become very cumbersome for large molecules. Many theoretical models, such as the wave function-based ab initio methods and the electronic density-based TDDFT approach, have been proposed to study the electronic excited states. However, high accuracy ab initio methods are computationally heavy, and simulations are limited to very small-sized systems. With the combination of its simplicity and relatively high accuracy, TDDFT has grown to be a preferred alternative and has been playing an increasingly important role on the study of the excited states. The implementation of analytical first-order energy derivatives of electronic excited states with respect to nuclear coordinates in many electronic structure software packages[28−39] makes it possible to calculate the equilibrium structure and the Stokes shift within the framework of TDDFT. The successful realization of the analytical calculation on the excited-state Hessian within TDDFT[40,41] has made the large-scale numerical calculations on the excited-state vibrational frequencies and other related physical quantities, such as the geometrical derivatives of the transition dipole moment become feasible for the medium-sized systems. However, TDDFT cannot explicitly yield the shifts and the rotational matrix. Fortunately, we have proposed a method to obtain those parameters in the investigation of absorption and emission spectra.[42−45] This technique can be straightforwardly used in the calculation of RRS.

To demonstrate the accuracy of the current integrated approaches: the time-dependent approach to RRS and the analytic energy derivative approach for TDDFT excited-state properties, we first calculate RRS spectra of phenoxyl radical since both its experimental[46] and theoretical[27] spectra are available. Then, we apply the present approaches to 2-Thiopyridone (2-TP) in water solution to reveal the contributions of the HT term and solvent on RRS. Finally, the integrated approaches will be applied to calculate the spectra of free base porphyrin (H2P). From the predicted RRS, we further reveal the detailed dependence of RRS intensities on the structure parameters, which may be helpful in realistic applications to choose suitable electronic structure methods, such as the theoretical model and basis sets.

The paper is organized as follows. In Section 2, we briefly outline the theoretical and computational details. The applications to a few selected systems are shown in Section 3. Section 4 is the concluding remarks.

2. THEORY AND COMPUTATIONAL DETAILS

2.1. Time-Dependent RRS Approach. It is known that the differential photon scattering cross section of RRS is given by the following:[24,47]

$$\sigma(\omega_I, \omega_S) \propto \frac{4\omega_I\omega_S^3}{9c^4} S(\omega_I, \omega_S) \tag{1}$$

Here, ω_I and ω_S denote the frequencies of the incident and scattering photons, respectively. c is the speed of light. The resonance Raman line shape $S(\omega_I,\omega_S)$ has a form,

$$S(\omega_I, \omega_S) = 2\pi \sum_{n,m} P(n)|\hat{e}_S\cdot\alpha_{mn}\cdot\hat{e}_I|^2\delta(\omega_S - \omega_I - \varepsilon_n + \varepsilon_m) \tag{2}$$

where the unit vectors $\hat{e}_I$ and $\hat{e}_S$ point along the polarization directions of the incident and scattered radiations. In eq 2, it is assumed that the molecule is initially excited by the incident radiation from the n-th vibrational state on the electronic ground state with the population distribution $P(n)$, and it is back to the same electronic state but with different vibrational state m by the scattering radiation. ε_n and ε_m are the corresponding vibrational energies. α_{mn} is the KHD polarizability tensor,[48,49]

$$\alpha_{mn} = \sum_k \left[\frac{\langle m|\mu^S|k\rangle\langle k|\mu^I|n\rangle}{\omega_{kn} - \omega_I - i\gamma} + \frac{\langle n|\mu^I|k\rangle\langle k|\mu^S|m\rangle}{\omega_{km} + \omega_I + i\gamma} \right] \tag{3}$$

where μ is the transition dipole moment, k represents all possible intermediate states, and γ is the damping constant for electronic state k. As the adiabatic energy gaps ω_{kn} between the k states and the initial n state are close to the laser frequency ω_I, these intermediate k states will make the dominant contribution to RRS. Under the "resonant" conditions, the contributions from the nonresonant electronic states (the second term in eq 3) can be neglected. Considering a single resonant intermediate electronic state $|e\rangle$, we get,

$$\alpha_{mn} = \sum_{k_e} \frac{\langle m|\mu_{eg}|k_e\rangle\langle k_e|\mu_{eg}|n\rangle}{\omega_{nk_e} - \omega_I - i\gamma} \tag{4}$$

where k_e represents the vibrational state, with the energy ε_{k_e}, on the resonant electronic excited state, and $\omega_{nk_e} = \omega_{eg} + \varepsilon_{k_e} - \varepsilon_n$. Under the FC approximation, the transition dipole moment μ_{eg} between the ground and excited electronic states is constant, assumed to be μ_0. Equation 4 exactly corresponds to the Albrecht's A term,[24]

$$\mathrm{FC} = A \equiv \alpha_{mn}^{\mathrm{FC}} = \mu_0^2 \sum_{k_e} \frac{\langle m|k_e\rangle\langle k_e|n\rangle}{\omega_{nk_e} - \omega_I - i\gamma} \tag{5}$$

As μ_{eg} explicitly depends on the coordinates of the vibrational normal modes, one may expand it with respect to the ground-state normal coordinates Q^g

$$\mu_{eg} = \mu_0 + \sum_l \frac{\partial\mu_{eg}}{\partial Q_l^g} Q_l^g + \cdots \tag{6}$$

where the sum l runs over all $3N - 6$ normal modes. With the appropriate substitutions, eq 4 now reads to first order in Q as follows:

$$\alpha_{mn} = A + B + C \tag{7}$$

where,

$$B = \mu_0 \sum_{k_e} \frac{\langle m|k_e\rangle\langle k_e|\sum_l \frac{\partial\mu_{eg}}{\partial Q_l^g} Q_l^g|n\rangle}{\omega_{nk_e} - \omega_I - i\gamma} + \mu_0 \sum_{k_e} \frac{\langle m|\sum_j \frac{\partial\mu_{eg}}{\partial Q_j^g} Q_j^g|k_e\rangle\langle k_e|n\rangle}{\omega_{nk_e} - \omega_I - i\gamma} \tag{8}$$

dx.doi.org/10.1021/ct300640c | J. Chem. Theory Comput. 2012, 8, 4474−4482

$$C = \sum_{k_e} \frac{\langle m|\sum_j \frac{\partial \mu_{eg}}{\partial Q_j^g} Q_j^g |k_e\rangle\langle k_e|\sum_l \frac{\partial \mu_{eg}}{\partial Q_l^g} Q_l^g |n\rangle}{\omega_{nk_e} - \omega_I - i\gamma} \quad (9)$$

Equations 8 and 9 are defined as Albrecht's B and C terms,[24] respectively. Then the HT contribution to the polarizability is to sum B and C, i.e., $HT = B + C$.

To numerically calculate the FC and HT terms, one has to know the FC overlap integrals $\langle n|k_e\rangle$ and its overlap with mode coordinates $\langle n|Q_l^g|k_e\rangle$. As mentioned in Section 1, however, we do not explicitly calculate these quantities. Alternatively, we transform α_{mn} into the time domain. For the FC (A) term, using Green's function,

$$G(x) = \frac{1}{x - H_e} = \sum_{k_e} |k_e\rangle \frac{1}{x - \hbar\omega_{k_e} - i\gamma} \langle k_e| \quad (10)$$

In the time domain, $G(x)$ can be conveniently calculated by the following:

$$G(x) = -i\int_0^\infty dt e^{ixt-\gamma t} G(t) \quad (11)$$

with the propagator $G(t) \equiv \exp(-iH_e t)$, where H_e represents vibrational Hamiltonian on the electronic excited state. With use of eqs 10 and 11, the FC term becomes,

$$\mathrm{FC} = i|\mu_0|^2 \int_0^\infty \langle m|\exp(-iH_e t)|n\rangle \exp[i((\omega_I - \omega_{eg} + \varepsilon_n) - \gamma)t]dt \quad (12)$$

It is seen that the sum-overstate has been replaced by the propagation of vibrational motions on the excited state Hamiltonian.

To concretely calculate the propagator $G_{mn}(t)(= \langle m|\exp(-iH_e t)|n_e\rangle)$, one needs to know the vibrational Hamiltonian, which can be assumed to be a collection of harmonic oscillators:

$$H_g = \frac{1}{2}\sum_j^N (P_j^{g2} + \omega_j^{g2} Q_j^{g2}),$$
$$H_e = \frac{1}{2}\sum_j^N (P_j^{e2} + \omega_j^{e2} Q_j^{e2}) \quad (13)$$

Here, P and Q are the momenta and coordinates of the normal modes. The normal-mode coordinates of ground and excited states are correlated by the Duschinsky rotation matrix $\overline{S}$ with $Q^e = \overline{S}Q^g + \overline{D}$. $\overline{D}$ is the displacement of the normal mode coordinates between the equilibrium configurations of the ground and excited electronic states. With definitions of $D_i = (\omega_j^g \overline{D}_j)^{1/2}$ and $S_{ij} = (\omega_i^e/\omega_j^g)^{1/2}\overline{S}_{ij}$, $G_{mn}(t)$ has an analytical solution for the j-th single-mode excitation from n to m,[19]

$$G_{mn}(t) = \sigma_0(t) W_{mn}(t) \quad (14)$$

with

$$\sigma_0(t) = |\Psi(t)|^{-1/2}\exp[D^T f(t) D] \quad (15)$$

$$W_{mn}(t) = (m!n!2^{m+n})^{-1/2}[\beta(t)]^{m+n}\Sigma_{k=0}^{k^*}\frac{(2k)!}{k!}\eta_{mnk} [\zeta(t)]^k \times H_{m+n-2k}[\lambda f(t) D/\beta(t)] \quad (16)$$

Here H_p are the Hermite polynomials, k^* is the integer part of $(m + n)/2$, and,

$$\eta_{mnk} = \Sigma_{q=0}^{2k}(-1)^q C_m^{2k-q} C_q^n,\ C_m^n = \frac{m!}{n!(m-n)!} \quad (17)$$

$$f(t) = -(S^{-1})^T U C_- \quad (18)$$

$$\beta(t) = \left[\frac{1}{2} - (UC_+(S^{-1})^T)_{jj}\right]^{1/2} \quad (19)$$

$$\zeta(t) = -\frac{1 - 2(VC_-(S^{-1})^T)_{jj}}{1 - 2(UC_+(S^{-1})^T)_{jj}} \quad (20)$$

$$\Psi(t) = \frac{1}{4}U^{-1}V^{-1} \quad (21)$$

with

$$C_\pm = 1 \pm \exp(-i\omega_e t),\ \lambda = \frac{\omega_e}{\omega_g} \quad (22)$$

$$U = (C_+(S^{-1})^T + C_- S)^{-1},\ V = (C_+ S + C_-(S^{-1})^T)^{-1} \quad (23)$$

For the HT term, we may still use the Green's function technique. In order to do this, we first write the mode coordinate as $Q_l = (\hbar/2\omega_l)^{1/2}(\hat{a}_l^+ + \hat{a}_l)$, where $\hat{a}_l^+$ and $\hat{a}_l$ are the second quantization creation and annihilation operators, respectively. As Q_l acts on a vibrational state $|m\rangle$, we have the following:

$$Q_l|m\rangle = \sqrt{\frac{\hbar}{2\omega_l}}(\sqrt{m_l + 1}\,|m + 1_l\rangle + \sqrt{m_l}|m - 1_l\rangle) \quad (24)$$

where $|m + p_l\rangle$ represents the vibrational state where the quantum number of l-th mode is added by p_l with the unchanged numbers for the left modes. Using eqs 10 and 11, the HT term becomes,

$$\begin{aligned}\mathrm{HT} = i\int_0^\infty \Bigg\{ & \mu_0 \sum_l \sqrt{\frac{\hbar}{2\omega_l}}\frac{\partial \mu_{eg}}{\partial Q_l^g}\Big[\sqrt{n_l + 1}\,G_{mn+1_l}(t) + \sqrt{n_l}\,G_{mn-1_l}(t)\Big] \\ & + \mu_0 \sum_j \sqrt{\frac{\hbar}{2\omega_j}}\frac{\partial \mu_{eg}}{\partial Q_j^g}\Big[\sqrt{m_j + 1}\,G_{m+1_j n}(t) + \sqrt{m_j}\,G_{m-1_j n}(t)\Big] \\ & + \sum_l \sqrt{\frac{\hbar}{2\omega_l}}\frac{\partial \mu_{eg}}{\partial Q_l^g}\sum_j \sqrt{\frac{\hbar}{2\omega_j}}\frac{\partial \mu_{eg}}{\partial Q_j^g} \Big[\sqrt{(n_l + 1)(m_j + 1)}\,G_{m+1_j n+1_l}(t) \\ & + \sqrt{(n_l + 1)m_j}\,G_{m-1_j n+1_l}(t) + \sqrt{n_l(m_j + 1)}\,G_{m+1_j n-1_l}(t) \\ & + \sqrt{n_l m_j}\,G_{m-1_j n-1_l}(t)\Big]\Bigg\}\exp[i((\omega_I - \omega_{eg} + \varepsilon_n) - \gamma)t]dt \end{aligned} \quad (25)$$

Now, it becomes clear that both FC and HT terms can be calculated from the Fourier transforms of the analytical expressions of propagator $G_{mn}(t)$ in time domain.

2.2. Computational Details for the Electronic Structure Parameters. To realistically predict RRS, in addition to the

dx.doi.org/10.1021/ct300640c | J. Chem. Theory Comput. 2012, 8, 4474−4482

derived time-dependent formulas of eqs 12 and 25, one needs to know the related electronic structure parameters, such as the equilibrium structures and vibrational frequencies of both the ground and excited states, as well as the excitation energies, transition dipole moments, and their geometrical derivatives, etc. These quantities can be, in principle, calculated from the electronic structure theory. However, it is well-known that the high-accuracy ab initio methods are still limited to very small-sized systems for the excited states. Herein, we calculate these electronic structure parameters with respect to TDDFT by striking a balance between computational accuracy and efficiency. Our newly developed analytical derivative approaches for the TDDFT excited-state energy[39−41] will be used to locate the minima of excited-state potential energy surfaces, and calculate the excited-state vibrational frequencies and the geometrical derivatives of the transition dipole moments. All of the electronic structure calculations for phenoxyl radical and H2P are finished with the locally modified Q-chem software program.[50] The electronic structure calculations for 2-TP in water solution are finished with Gaussian 09.[51] The solvent effect is considered by the polarized continuum overlapping spheres model. The hybrid DFT exchange-correlation functional B3LYP is adopted.

The geometrical derivatives of the transition dipole moments can be evaluated as $\mu^x_{ge} = \mathrm{Tr}(\delta\rho^x\mu) + \mathrm{Tr}(\delta\rho\mu^x)$. Here $\delta\rho$ and μ are the transition density matrix and the dipole moment matrix in the representations of molecular orbitals or atomic orbitals, respectively. Observably, μ^x_{ge} is the reference geometry-dependent. In the analytical calculation of the excited-state Hessian, $\delta\rho^x$ has to be evaluated.[40,41] Therefore, the computational time is saved if one evaluates μ^x_{ge} accompanied with the calculation of excited-state Hessian at the excited-state equilibrium structures. However, in this work, we calculate the transition dipole moments at the molecular ground-state equilibrium structure, and therefore we transition the dipole moment in terms of the ground-state normal modes. Its geometrical derivatives are subsequently calculated at the ground-state equilibrium conformation. Anyway, there is no doubt that one can expand the transition dipole moment in terms of the excited-state normal modes and calculate the concerned physical quantities at the reference geometry of the excited state. In this case, the expressions of FC and HT terms in time-domain will be slightly different with eqs 12 and 25.

The other key step left is to obtain the displacement D for each mode and Duschinsky rotation matrix S. In the practical implementation, one may start from the relationship between the Cartesian coordinates of the optimized ground and excited states by,[42]

$$x_g = x_e + \Delta x \tag{26}$$

where x_g and x_e represent the mass-weighted Cartesian coordinates of the ground and excited states, respectively. Δx is the corresponding shift. The normal mode coordinates Q are transformed from Cartesian coordinates x as follows:

$$Q = Lx \tag{27}$$

where L is the transformation matrix. It is obtained from the diagonalization of the Hessian matrix K by the following:

$$L^T K L = \omega^2 \tag{28}$$

where ω are the frequencies. By using eqs 27 and 26 can be cast into the following:

$$Q_g = L_g L_e^T Q_e + L_g \Delta x \tag{29}$$

where L_g and L_e correspond to the transform matrix for the ground and excited states, respectively, and $L_g L_e^T (= \overline{S})$ is Duschinsky rotation matrix. $\overline{D}$ is thus obtained from $L_e \Delta x$. And then, we get the derivatives of the transition dipole moments with respect to the normal modes of reference states as $(\partial\mu_{eg}/\partial Q) = L^T(\partial\mu_{eg}/\partial x)$.

3. APPLICATIONS

In the realistic applications, we choose a few of selected systems: the phenoxyl radical in the gas phase, the 2-thiopyridone in water solution and free-base porphyrin. The former two molecules have the experimental data or the calculated results from the frequency domain, which allow for a critical comparison of the accuracy of the present computations. The last H2P molecule has been demonstrated that the strong HT effect plays a significant role in its absorption and emission spectra.[52,53] It is interesting to see how large a role the HT effect plays on the RR spectral intensity. Here we perform a calculation on RR spectra of H2P with the excitation energies corresponding to the lowest two singlet excited states.

In the calculation of the HT term in eq 25, the single mode excitation, e.g., $j = l$, is considered and the multimode combination bands are not included. The damping parameter γ in eq 3 strongly depends on the lifetime of excited state. We yield it by fitting the experimental absorption linewidths as shown in Supporting Information, SI. As a result, the reasonable damping parameters of 100, 300, and 300 cm^{-1} are used for phenoxyl radical, 2-TP in water solution and H2P molecules, respectively. As Section 2.1 shown, Raman scattering is described by a polarizability tensor, $\alpha(\omega_I,\omega_S)$, which has nine elements. In this work, we treat the case of the linearly polarized excitation with detection of all scattered polarizations in a direction perpendicular to the incident polarization. The Raman differential cross section has finally been calculated as eq 3 in ref 54.

Many theoretical works[16,19−21] have shown that the Duschinsky rotation significantly affects the RRS intensity. We also calculate RRS of the three molecules with and without the inclusion of Duschinsky rotation. The results are shown in Figure S2 in the SI. It is found that the Dschinsky rotation effect plays a significant role on the RRS of Phenoxyl Radical and 2-TP molecule, whereas its effect is weak on H2P. Herein, we only focus on the analysis of HT effect.

3.1. Phenoxyl Radical in the Gas Phase. To determine the resonant excitation states involved in RRS, we first show the vertical excitation energies and oscillator strengths of lowest-lying doublet excited states to see which excited-state energy is close to that of incident photons in the RRS experiment. The calculation is finished at TD-B3LYP/6-311+G(d,p) theoretical level. The excitation energies of lowest-lying three doublet excited states are 1.0557(0.0), 2.3417(0.0054), and 3.5641(0.0313) eV, respectively. The data in the parentheses denote the oscillator strengths. It appears that the excitation wavelength of 399 nm used in the RRS experiments[46] is in resonance with the absorption from $S_0 \rightarrow S_3$.[55] Comparison of the experiment and theory for the excitation energy is made. The error is visible. For example, the calculated adiabatic excitation energy between S_0 and S_3 is 366.6 nm (see Table 1), which is about 30 nm smaller than the experimental value of 396.83 nm.[55] It has been shown that TD-B3LYP can reasonably produce the spectral line shape of vibrationally resolved absorption spectrum with center frequency corresponding to $S_0 \rightarrow S_3$ transition.[27] Here, we thus use TD-B3LYP to calculate the geometrical or electronic structure parameters required by the expression of RRS.

Table 1. Calculated SCF Energies E_{scf}, Vertical Excitation Energies VE and Transition Dipole Moments at Different Equilibrium Geometries of Ground State (S_0) and Third Excited State (S_3)[a]

		S_3				
			transition dipole moments			
geom	E_{scf} (a.u.)	VE (nm)	x	y	z	exp (nm)
S_0	−306.913377	347.87	0.0000	0.0000	−0.5989	396.83
S_3	−306.907163	385.94	0.0000	0.0000	−0.7141	

[a]"Geom" denotes the reference geometrical structure of the state. The comparison is made with experimental excitation energy.

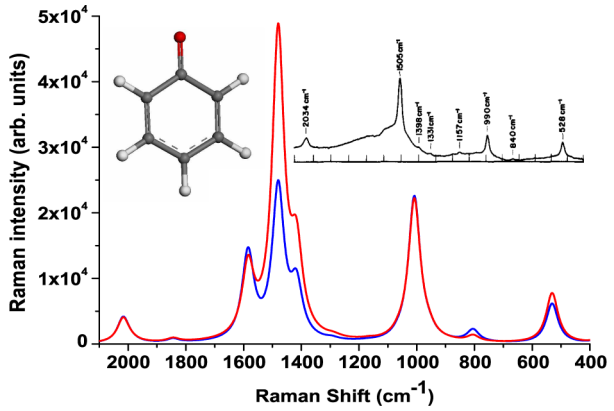

Figure 1. Calculated RRS of Phenoxyl radical with HT (red line) and without HT contribution (blue line) corresponding to resonance excitation $S_0 \rightarrow S_3$. The calculated spectra apply a damping factor of γ = 100 cm^{-1} and Lorentz broadening of 25 cm^{-1}. The insert shows the experimental RRS with an incident wavelength of 399 nm.

Figure 1 displays the experimental and the calculated RRS with the current time-dependent approach. The calculated RRS adopts an incident wavelength of 366.6 nm, which exactly equals to the adiabatic excitation energy of S_3. Compared with the experimental result, our calculation nicely yields the positions and the relative magnitude order of band intensities of RRS. A major band at 1500 cm^{-1} (1505 cm^{-1} in experiment), a few of relatively weak bands at 528, 840, 1007, 1331, 1398, and 2034 cm^{-1} are well produced by our calculations. The experiment shows that a shoulder appears at near 1600 cm^{-1}, which is much weaker than the major band at 1505 cm^{-1}. The calculation based on the SOS method overestimated the intensity of the band at 1584 cm^{-1}.[27] Observably, the current time-dependent approach gives more reasonable description to this band. The larger error yielded by the SOS method[27,56] may come from the neglect of some intermediate vibrational states which play an important role on the RRS of Phenoxyl Radical or the inaccurate geometrical derivatives of transition dipole moments, which are calculated by the finite-difference method in ref 27.

Table S1 in the SI lists the derivatives of transition dipole moments with respect to the normal modes. The relatively large values of the derivatives give rise to the significant HT effect. The HT effect conspicuously enhances the RRS intensity at 1500 cm^{-1}, reduces that at 1600 cm^{-1}, and makes the overall spectral line shape agree better with the experiment than the RRS without HT contributions. Our results verify that the time-dependent approach to RRS coupled with the analytical calculations on the excited-state-related geometrical properties is an effective integrated approach to describe vibronic progressions.

3.2. 2-Thiopyridone. Typically, vibrational signatures are sensitive to electron-shifts and changes in environment and solvents may explicitly change RRS. Here, we investigate the RRS of 2-TP in gas phase and water solution with the present approaches. The electronic structure calculations are finished by TD-B3LYP/6-311+G(d,p). The solvent effect is considered by the polarized continuum overlapping spheres model. In water solution, the calculation yields the vertical excitation energies 379.23(0.0002), 353.09(0.1285), 299.32(0.0002), and 280.57-(0.3512) eV for four lowest-lying singlet excited states, respectively. It is noted that the experimental measurement shows two strong absorption bands at 341.6 nm (A-band) and 270.4 nm (B-band) for 2-TP in water solution,[57,58] which are consistent with the calculated excitation energies of the second and fourth excited states. In the RRS measurement,[58] 266 nm excitation wavelength is used, corresponding to the resonance with the B-band absorption of 2-TP (see Table 2). We then calculate the corresponding RRS.

The experimental RRS shows four strong 2-TP ring-stretching band at 731, 994, 1565, and 1614 cm^{-1} as well as four C═C/N stretch band at 1167, 1233, 1445, and 1505 cm^{-1}, which have been assigned by Du et al.[58] The significant HT effects are arisen from the larger geometrical alternations after the electronic excitation, which are manifested by the larger derivatives of the transition dipole moment (See Table S2 in the SI) and coordinate shift Δx. Comparing the ground-state and excited-state equilibrium conformations, we observe that the atom S is explicitly out of molecular plane after electronic excitation. In comparison with the experimental results, the calculated RRS spectra blue shift slightly. It is known that the calculated harmonic vibrational frequencies are typically larger than the observed values.[59] A major source of this deviation arises from the incomplete incorporation of the electron correlation and the use of finite basis sets, as well as the neglect of anharmonicity effects in the theoretical calculations. Therefore, here we scale the calculated harmonic frequencies of the ground-state and excited-state with a scaling factor of 0.98. The scaled frequencies are applied to reproduce the RR spectra in Figure 2(b). It is explicit that after applying the scaling factors to the calculated frequencies, the relative positions of RR spectral peaks agree better with the experimental measurement. Here, the calculated RR spectral cross sections have been normalized to yield the experimental intensity at 1505 cm^{-1}.

For the comparison, the RRS of 2-TP in gas phase is plotted in Figure 3. We observe that a significant difference appears in the calculated and experimental RR spectra. The RR spectral intensities in the low-frequency range are significantly overestimated. It seems that the solution greatly restricts the vibration of low-frequency modes. The solvent effect on RRS of 2-TP is conspicuous. With the solvent effect is taken into account, the calculated RRS compares more favorably with the available experimental spectrum.

3.3. Free-Base Porphyrin (H2P). In this subsection, we display the application to H2P. The majority of free-base porphyrin shows very characteristic absorption of two sets of

Table 2. Calculated SCF Energies E_{scf}, Vertical Excitation Energies VE and Transition Dipole Moments at the Equilibrium Geometries of the Ground State (S_0) and Fourth Excited State (S_4) by TD-B3LYP in Gas Phase and Water Solution[a]

	gas					water					
		S_4					S_4				
			transition dipole moments					transition dipole moments			
geom	E_{scf} (a.u.)	VE (nm)	x	y	z	E_{scf} (a.u.)	VE (nm)	x	y	z	exp (nm)
S_0	−646.574939	284.04	−1.5308	−0.4027	0.1088	−646.590252	280.57	−1.9563	−0.5122	0.1388	270.4
S_4	−646.541954	392.56	1.3998	0.2444	0.1245	−646.578059	314.12	−1.9247	−0.4827	−0.0156	

[a]The comparison is made with experimental data.

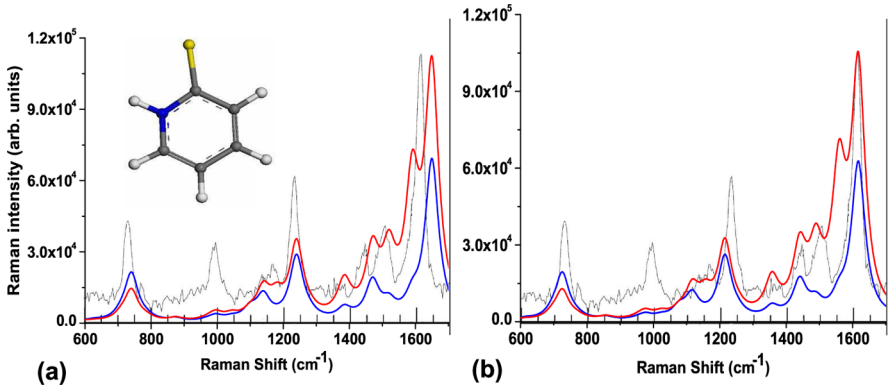

Figure 2. Calculated RR spectra of 2-TP in water solution with HT (red line) and without HT contribution (blue line). The right panel demonstrates the RRS with the scaled vibrational frequencies (scaling factor: 0.98). A damping factor of γ = 300 cm^{-1} and Lorentz broadening factor of 25 cm^{-1} are applied. The experimental RRS with an incident wavelength of 266 nm is also shown for comparison (black thin line).

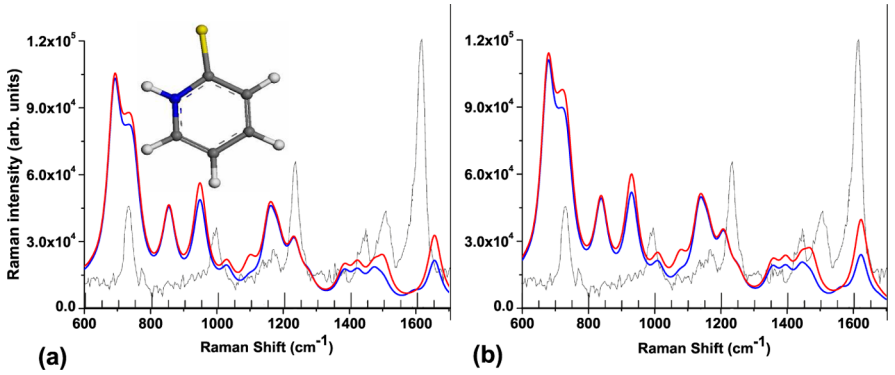

Figure 3. Calculated RR spectra of 2-TP in gas phase with HT (red line) and without HT contribution (blue line). The right panel demonstrates the RRS with the scaled vibrational frequencies (scaling factor: 0.98). A damping factor of γ = 100 cm^{-1} and Lorentz broadening factor of 25 cm^{-1} are applied.

bands in the ranges of 400−450 nm and 550−700 nm. The first sets of bands in the UV range are called the B band or Soret band (strongly allowed) and the lower energy sets in the optical range are the Q bands (quasi-allowed).[60] The vibronic structures in Q bands of free-base porphyrins are experimentally observed. The four lines in the Q-band are $Q_x(0,0)$, $Q_x(0,1)$, $Q_y(0,0)$, and $Q_y(0,1)$ in the increasing order of energy. To check the performance of TDDFT on this molecule, we use TD-B3LYP to calculate the vertical excitation energies and transition dipole moments of H2P at the equilibrium geometries of both the ground and excited states. The results are displayed in Table 3. The experimental excitation energies reported at 1.98−2.02 and 2.33−2.42 eV.[60] TD-B3LYP/6-311G(d) yields the theoretical adiabatic energy gap of 0.16 eV between Q_x and Q_y excitations and underestimates the energy gap.

A lot of works have been devoted to investigate the vibrationally resolved absorption and emission spectra of H2P under harmonic approximation with the inclusion of mode mixing and HT effect.[52,53,61] It has been verified that the HT effect must be taken into account to produce the correct vibronic spectra because the Q bands are only quasi-allowed. Here we apply the time-dependent approach to calculate the RR spectra which are corresponding to the absorption maxima of Q_x and Q_y. The results are shown in Figures 4 and 5. The most evident differences are introduced by HT effects. The predicted spectral lineshapes, peak intensities, and positions change remarkably accompanying by the appearance/disappearance of some peaks as the computational model varies. With the introduction of HT terms, the bands in the range of higher frequencies are significantly enhanced. Here, the adiabatic energy gaps between the ground and excited states are taken as the incident frequencies.

Since the electronic and geometrical structures of molecules are affected by the theoretical modes and basis sets adopted by the electronic structure calculations, they subsequently affect RRS.

Table 3. Calculated SCF Energies E_{scf}, Vertical Excitation Energies VE and Transition Dipole Moments at the Equilibrium Geometries of S_0, S_1 and S_2 States with Different Theoretical Levels and Basis Sets

			S_1				S_2			
				transition dipole moments				transition dipole moments		
geom	model/basis	E_{scf} (a.u.)	VE (eV)	x	y	z	VE (eV)	x	y	z
S_0	TDDFT/6-31G(d)	−989.551120	2.2802	−0.0093	0.0002	0.0000	2.4417	0.0002	−0.0143	0.0000
	TDA/6-311G(d)	−989.758447	2.3246	−0.0447	0.0002	0.0000	2.5154	0.0011	0.1125	0.0000
	TDDFT/6-311G(d)	−989.758447	2.2809	0.0014	−0.0004	0.0000	2.4321	0.0004	0.0301	0.0000
S_1	TDDFT/6-31G(d)	−989.550365	2.2413	−0.1497	0.0010	0.0000				
	TDA/6-311G(d)	−989.757843	2.2928	−0.0557	−0.0003	0.0000				
	TDDFT/6-311G(d)	−989.757719	2.2418	0.1392	−0.0007	0.0000				
S_2	TDDFT/6-311G(d)	−989.550737					2.4115	−0.0002	−0.0444	0.0000

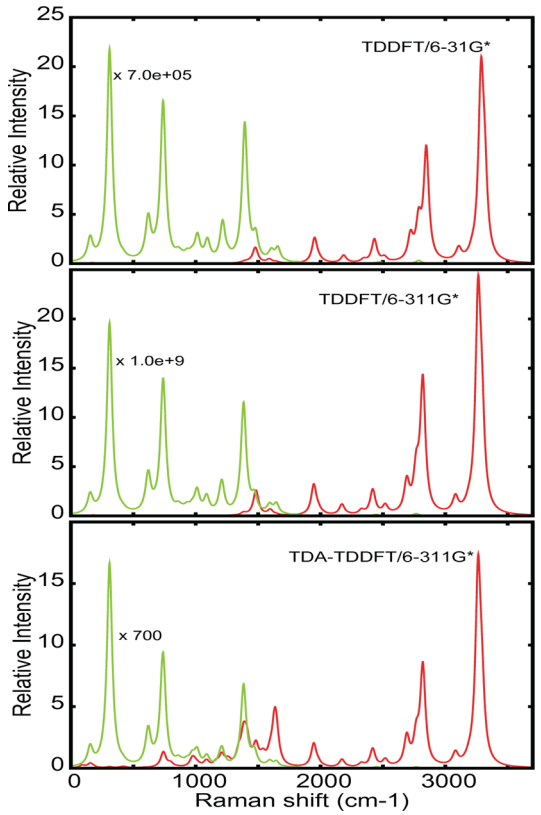

Figure 4. Calculated RR spectra of H2P with HT (red line) and without HT contribution (green line) corresponding to the electronic excitation of $S_0 \rightarrow S_1$. A damping factor of $\gamma = 300$ cm^{-1} and Lorentz broadening of 25 cm^{-1} are applied. To have a comparison with the intensities of RRS with HT contribution, these of RRS without HT terms are amplified.

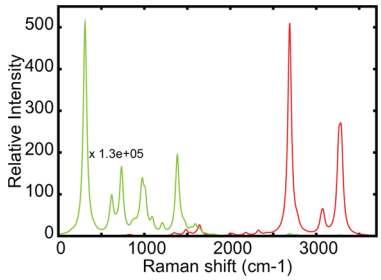

Figure 5. Calculated RR spectra of H2P with HT (red line) and without HT contribution (green line) corresponding to the excitation of $S_0 \rightarrow S_2$ at TDDFT/6-311G*.

In the following, we therefore employ the different theoretical modes and basis sets to calculate the electronic structure parameters. At first, we check the effect of basis sets on RRS. By comparing the results with the different basis sets as shown in Figure 4, we find that both the 6-31G* and 6-311G* basis sets yield the similar spectral lineshapes, but slightly different peak positions and remarkably different peak intensities in the FC regime. The HT effect on RRS is similar. The bands at the frequencies larger than 1500 cm^{-1} are significantly enhanced in comparison with those without HT effect and finally lead to the RRS yielded by larger basis set is similar to that by smaller basis set. It indicates that the HT effect complements the deficiencies of small basis set on the geometrical and electronic structures. Usually, larger basis set is required to perform the electronic structure calculation since in the simulation of RRS, the excited electronic state is related.

Tamm−Dancoff approximation (TDA), which ignores all of the B matrix elements in the TDDFT working equation,[62] has been regarded as an algorithmically simpler alternative to full TDDFT. TDA-TDDFT significantly simplifies the algebra and the associated algorithms to obtain the excitation energies and introduces only very small errors in the calculated excitation energies except for those states having the triplet near-instability problems.[62] This is a consequence of the fact that B matrix plays a very minor role, in fact only a negligibly small role, in the TDDFT excitation energies. It is interesting to see whether TDA-TDDFT is suited for the description of excited-state properties. Comparing the RRS spectra obtained by the full TDDFT and TDA-TDDFT, the relative intensities of RRS and HT effect on RRS are remarkably different. TDA approximation to full TDDFT produces a quite different transition dipole moments and the geometrical derivatives of transition dipole moments in comparison with full TDDFT, which subsequently lead to the different RR spectral lineshapes, especially the remarkably different relative magnitude order of band intensities. TDA-TDDFT is accurate enough for the excited-state frequency calculation in contrast to full TDDFT calculation.[41] However, due to the well-known fact that TDA ignores all the B matrix elements in the TDDFT working equation and leads to the oscillator strength sum rule broken down. Therefore, TDA-TDDFT yields incorrect transition dipole moments and their geometrical derivatives. For example, with the optimized S_1 state geometry, the vertical excitation energy yielded by TDDFT/6-311G(d) is only 0.05 eV smaller than that by TDA/6-311G(d), but its x-component of transition dipole moment is twice that of TDA, but with opposite direction. Therefore, TDA-TDDFT may not be particularly well suited to describe the excited-state properties. The calculated RRS with the absorption maximum of $S_0 \rightarrow S_2$ has been shown in Figure 5. Comparing the spectra of Q_x with Q_y, the differences are visible. The contribution of HT term to the spectra of Q_x and Q_y bands is also different.

dx.doi.org/10.1021/ct300640c | J. Chem. Theory Comput. 2012, 8, 4474−4482

4. CONCLUSIONS

We have presented a computationally effective time-dependent approach to resonance Raman spectroscopy with inclusion of Herzberg−Teller contribution and Duschinsky rotation effect. The proposed analytic expression for RRS in the time domain avoids summation over intermediate vibrational states compared to traditional approaches in the frequency domain. As shown in the analytical expression of RRS, the molecular electronic and geometrical properties of the pertinent states are related. In this work, we have used our recently developed analytic energy derivative approaches for the TDDFT excited states. The analytic approaches to these physical quantities guarantee higher computational efficiency and accuracy than the conventional finite-difference method. The current integrated dynamic and electronic structure approaches are therefore well suited to simulate the RRS of large molecules. It is also ready to extend them to calculate the vibrationally resolved absorption and emission spectra of large molecules with the inclusion of HT contribution and mode-mixing effect.

In order to demonstrate the accuracy of the proposed methods, we have calculated the RRS of a few conjugated systems, the phenoxyl radical in the gas phase, the 2-Thiopyridone in water solution, and free base porphyrin. The obtained results are consistent with the experimental measurements and other theoretical results calculated from the frequency domain. In addition, as expected, the basis sets, theoretical models, and reference geometries play a significant role on the electrotonic and geometrical structures of the molecules, succeedingly on RRS. The HT effect seems to complement the deficiencies of the small basis set on the parameters of geometrical and electronic structures, leading to the insignificant basis-set effect on RRS of H2P when the HT contribution is taken into account. The TDA approximation to TDDFT is not suitable for the vibrationally resolved spectroscopies.

■ ASSOCIATED CONTENT

Ⓢ Supporting Information

Absorption spectra, RR spectra with and without including Duschinsky rotation, the optimized ground and excited state geometries, and the derivatives of transition dipole moment with respect to ground-state normal mode coordinates. This material is available free of charge via the Internet at http://pubs.acs.org.

■ AUTHOR INFORMATION

Corresponding Author

*E-mail: liangwz@xmu.edu.cn.

Notes

The authors declare no competing financial interest.

■ ACKNOWLEDGMENTS

Financial support from National Science Foundation of China (Grant No. 20833003 and No:21073168), the National Basic Research Program of China (Grant No. 2011CB808501) are acknowledged. The partial numerical calculations in this work have been done on the supercomputing system in the Supercomputing Center of University of Science and Technology of China.

■ REFERENCES

(1) Myers, A. B. Resonance Raman Intensities and Charge-Transfer Reorganization Energies. *Chem. Rev.* **1996**, *96*, 911−926.
(2) Myers, A. B. Resonance Raman Intensity Analysis of Excited-State Dynamics. *Acc. Chem. Res.* **1997**, *30*, 519−527.
(3) McHale, J. L. Subpicosecond Solvent Dynamics in Charge-Transfer Transitions: Challenges and Opportunities in Resonance Raman Spectroscopy. *Acc. Chem. Res.* **2001**, *34*, 265−272.
(4) Hupp, J. T.; Williams, R. D. Using Resonance Raman Spectroscopy to Examine Vibrational Barriers to Electron Transfer and Electronic Delocalization. *Acc. Chem. Res.* **2001**, *34*, 808−817.
(5) Spiro, T. G.; Stein, P. Resonance Effect in Vibrational Scattering from Complex Molecules. *Annu. Rev. Phys. Chem.* **1977**, *28*, 501−521.
(6) Warshel, A. Interpretation of Resonance Raman Spectra of Biological Molecules. *Annu. Rev. Biophys. Bioeng.* **1977**, *6*, 273−300.
(7) Champion, P. M.; Albrecht, A. C. Resonance Raman Scattering: The Multimode Problem and Transform Methods. *Annu. Rev. Phys. Chem.* **1982**, *33*, 353−376.
(8) Wächtler, M.; Guthmuller, J.; González, L.; Dietzek, B. Analysis and Characterization of Coordination Compounds by Resonance Raman Spectroscopy. *Coord. Chem. Rev.* **2012**, *256*, 1479−1508.
(9) Sharp, T. E.; Rosenstock, H. M. Franck-Condon Factors for Polyatomic Molecules. *J. Chem. Phys.* **1963**, *41*, 3453−3463.
(10) Kupka, H.; Cribb, P. H. Multidimensional Franck-Condon Integrals and Duschinsky Mixing Effects. *J. Chem. Phys.* **1986**, *85*, 1303−1315.
(11) Ruhoff, P. T. Recursion Relations for Multi-Dimensional Franck-Condon Overlap Integrals. *Chem. Phys.* **1994**, *186*, 355−374.
(12) Doktorov, E. V.; Malkin, I. A.; Man'ko, V. I. Dynamical Symmetry of Vibronic Transitions in Polyatomic Molecules and Frank-Condon Principle. *J. Mol. Spectrosc.* **1977**, *64*, 302−326.
(13) Doktorov, E. V.; Malkin, I. A.; Man'ko, V. I. Dynamical Symmetry of Vibronic Transitions in Polyatomic Molecules and The Franck-Condon Principle. *J. Mol. Spectrosc.* **1975**, *56*, 1−20.
(14) Peluso, A.; Santoro, F.; Del Re, G. Vibronic Coupling in Electronic Transitions with Significant Duschinsky Effect. *Int. J. Quantum Chem.* **1997**, *63*, 233−244.
(15) Heller, E. J.; Lee, S.-Y. Time-Dependent Theory of Raman Scattering. *J. Chem. Phys.* **1979**, *71*, 4777−4788.
(16) Heller, E. J.; Sundberg, R. L.; Tannor, D. J. Polyatomic Raman Scattering for General Harmonic Potentials. *J. Phys. Chem.* **1982**, *86*, 1822−1833.
(17) Heller, E. J.; Tannor, D. J. Polyatomic Raman Scattering for General Harmonic Potentials. *J. Chem. Phys.* **1982**, *77*, 202−218.
(18) Duschinsky, F. *Acta Physicochim. URSS* **1937**, *7*, 551.
(19) Yan, Y. J.; Mukamel, S. Eigenstate-Free, Green Function, Calculation of Molecular Absorption and Fluorescence Line Shapes. *J. Chem. Phys.* **1986**, *85*, 5908−5923.
(20) Islampour, R.; Hayashi, M.; Lin, S. H. On the Calculation of Resonance Raman Spectra. *J. Raman Spectrosc.* **1997**, *28*, 331−338.
(21) Dehestani, M.; Islampour, R. Effects of Distortion-Rotation of Potential Energy Surfaces on Absorption and Resonance Raman Cross Sections of Trans-Stilbene Molecule. *Int. J. Quantum Chem.* **2005**, *103*, 119−126.
(22) Silverstein, D. W.; Jensen, L. Vibronic Coupling Simulations for Linear and Nonlinear Optical Processes: Simulation Results. *J. Chem. Phys.* **2012**, *136*, 064110.
(23) Silverstein, D. W.; Jensen, L. Vibronic Coupling Simulations for Linear and Nonlinear Optical Processes: Theory. *J. Chem. Phys.* **2012**, *136*, 064111.
(24) Albrecht, A. C. On the Theory of Raman Intensities. *J. Chem. Phys.* **1961**, *34*, 1476−1484.
(25) Albrecht, A. C.; Hutley, M. C. On the Dependence of Vibrational Raman Intensity on the Wavelength of Incident Light. *J. Chem. Phys.* **1971**, *55*, 4438−4443.
(26) Hizhnyakov, V.; Tehver, I. Transform Method in Resonance Raman Scattering with Quadratic Franck−Condon and Herzberg−Teller Interactions. *J. Raman Spectrosc.* **1988**, *19*, 383−388.
(27) Santoro, F.; Cappelli, C.; Barone, V. Effective Time-Independent Calculations of Vibrational Resonance Raman Spectra of Isolated and Solvated Molecules Including Duschinsky and Herzberg−Teller Effects. *J. Chem. Theory Comput.* **2011**, *7*, 1824−1839.

(28) Caillie, C. V.; Amos, R. D. Geometric Derivatives of Excitation Energies Using SCF and DFT. *Chem. Phys. Lett.* **1999**, *308*, 249−255.
(29) Caillie, C. V.; Amos, R. D. Geometric Derivatives of Density Functional Theory Excitation Energies Using Gradient-Corrected Functionals. *Chem. Phys. Lett.* **2000**, *317*, 159−164.
(30) Hutter, J. Excited State Nuclear forces from The Tamm−Dancoff Approximation to Time-Dependent Density Functional Theory within The Plane Wave Basis Set Framework. *J. Chem. Phys.* **2003**, *118*, 3928−3934.
(31) Furche, F.; Ahlrichs, R. Adiabatic Time-Dependent Density Functional Methods for Excited State Properties. *J. Chem. Phys.* **2002**, *117*, 7433−7447.
(32) Rappoport, D.; Furche, F. Analytical Time-Dependent Density Functional Derivative Methods within The RI-J Approximation, An Approach to Excited States of Large Molecules. *J. Chem. Phys.* **2005**, *122*, 064105.
(33) Scalmani, G.; Frisch, M. J.; Mennucci, B.; Tomasi, J.; Cammi, R.; Barone, V. Geometries and Properties of Excited States in The Gas Phase and in Solution: Theory and Application of A Time-Dependent Density Functional Theory Polarizable Continuum Model. *J. Chem. Phys.* **2006**, *124*, 094107.
(34) Thorvaldsen, A. J.; Ruud, K.; Kristensen, K.; Jøgensen, P.; Coriani, S. A Density Matrix-Based Quasienergy Formulation of the Kohn−Sham Density Functional Response Theory Using Perturbation- and Time-Dependent Basis Sets. *J. Chem. Phys.* **2008**, *129*, 214108.
(35) Coriani, S.; Kærgaard, T.; Jørgensen, P.; Ruud, K; Huh, J.; Berger, R. An Atomic-Orbital-Based Lagrangian Approach for Calculating Geometric Gradients of Linear Response Properties. *J. Chem. Theory Comput.* **2010**, *6*, 1028−1047.
(36) Liu, F.; Gan, Z.; Shao, Y. H.; Hsu, C. P.; Dreuw, A.; Head-Gordon, M.; Miller, B. T.; Brooks, B. R.; Yu, J. G.; Furlani, T. R.; Kong, J. A Parallel Implementation of The Analytic Nuclear Gradient for Time-Dependent Density Functional Theory within The Tamm−Dancoff Approximation. *Mol. Phys.* **2010**, *108*, 2791−2800.
(37) Chiba, M.; Tsuneda, T.; Hirao, K. Excited State Geometry Optimizations by Analytical Energy Gradient of Long-Range Corrected Time-Dependent Density Functional Theory. *J. Chem. Phys.* **2006**, *124*, 144106.
(38) Cammi, R.; Mennucci, B.; Tomasi, J. Fast Evaluation of Geometries and Properties of Excited Molecules in Solution: A Tamm−Dancoff Model with Application to 4-Dimethylaminobenzonitrile. *J. Phys. Chem. A* **2000**, *104*, 5631−5637.
(39) Liu, J.; Liang, W. Z. Molecular-Orbital-Free Algorithm for The Excited-State Force in Time-Dependent Density Functional Theory. *J. Chem. Phys.* **2011**, *134*, 044114.
(40) Liu, J.; Liang, W. Z. Analytical Hessian of Electronic Excited States in Time-Dependent Density Functional Theory with Tamm−Dancoff Approximation. *J. Chem. Phys.* **2011**, *135*, 014113.
(41) Liu, J.; Liang, W. Z. Analytical Approach for The Excited-state Hessian in Time-Dependent Density Functional Theory: Formalism, Implementation, and Performance. *J. Chem. Phys.* **2011**, *135*, 184111.
(42) Liang, W. Z.; Zhao, Y.; Sun, J.; Song, J.; Hu, S. L.; Yang, J. L. Electronic Excitation of Polyfluorenes: A Theoretical Study. *J. Phys. Chem. B* **2006**, *110*, 9908−9915.
(43) Gao, F.; Zhao, Y.; Liang, W. Z. Vibrationally Resolved Absorption and Emission Spectra of Rubrene Multichromophores: Temperature and Aggregation Effects. *J. Phys. Chem. A* **2009**, *113*, 12847−12856.
(44) Gao, F.; Zhao, Y.; Liang, W. Z. Vibronic Spectra of Perylene Bisimide Oligomers: Effects of Intermolecular Charge-Transfer Excitation and Conformational Flexibility. *J. Phys. Chem. B* **2011**, *115*, 2699−2708.
(45) Gao, F.; Liang, W. Z.; Zhao, Y. Theoretical Studies of Vibrationally Resolved Absorption and Emission Spectra: From a Single Chromophore to Multichromophoric Oligomers/Aggregates. *Sci. China Chem.* **2010**, *53*, 297−309.
(46) Tripathi, G. N. R.; Schuler, R. H. The Rresonance Raman Spectrum of Phenoxyl Radical. *J. Chem. Phys.* **1984**, *81*, 113−121.
(47) Long, D. A. *The Raman Effect*; Wiley: Chichester, U.K., 2002.
(48) Kramers, H. A.; Heisenberg, W. Über Die Streuung Von Strahlung Durch Atome. *Z. Phys.* **1925**, *31*, 681−708.
(49) Dirac, P. A. M. The Quantum Theory of Dispersion. *Proc. R. Soc. London, Ser. A* **1927**, *114*, 710−728.
(50) Shao, Y.; Molnar, L. F.; Jung, Y.; Kussmann, J.; Ochsenfeld, C.; Brown, S. T.; Gilbert, A. T. B.; Slipchenko, L. V.; Levchenko, S. V.; O'Neill, D. P.; DiStasio, R. A.; Lochan, R. C.; Wang, T.; Beran, G. J. O.; Besley, N. A.; Herbert, J. M.; Lin, C. Y.; Van Voorhis, T.; Chien, S. H.; Sodt, A.; Steele, R. P.; Rassolov, V. A.; Maslen, P. E.; Korambath, P. P.; Adamson, R. D.; Austin, B.; Baker, J.; Byrd, E. F. C.; Dachsel, H.; Doerksen, R. J.; Dreuw, A.; Dunietz, B. D.; Dutoi, A. D.; Furlani, T. R.; Gwaltney, S. R.; Heyden, A.; Hirata, S.; Hsu, C. P.; Kedziora, G.; Khalliulin, R. Z.; Klunzinger, P.; Lee, A. M.; Lee, M. S.; Liang, W.; Lotan, I.; Nair, N.; Peters, B.; Proynov, E. I.; Pieniazek, P. A.; Rhee, Y. M.; Ritchie, J.; Rosta, E.; Sherrill, C. D.; Simmonett, A. C.; Subotnik, J. E.; Woodcock, H. L.; Zhang, W.; Bell, A. T.; Chakraborty, A. K.; Chipman, D. M.; Keil, F. J.; Warshel, A.; Hehre, W. J.; Schaefer, H. F.; Kong, J.; Krylov, A. I.; Gill, P. M. W.; Head-Gordon, M. *Phys. Chem. Chem. Phys.* **2006**, *8*, 3172.
(51) Frisch, M. J.; Trucks, G. W.; Schlegel, H. B.; Scuseria, G. E.; Robb, M. A.; Cheeseman, J. R.; Scalmani, G.; Barone, V.; Mennucci, B.; Petersson, G. A.; Nakatsuji, H.; Caricato, M.; Li, X.; Hratchian, H. P.; Izmaylov, A. F.; Bloino, J.; Zheng, G.; Sonnenberg, J. L.; Hada, M.; Ehara, M.; Toyota, K.; Fukuda, R.; Hasegawa, J.; Ishida, M.; Nakajima, T.; Honda, Y.; Kitao, O.; Nakai, H.; Vreven, T.; Montgomery, Jr., J. A.; Peralta, J. E.; Ogliaro, F.; Bearpark, M.; Heyd, J. J.; Brothers, E.; Kudin, K. N.; Staroverov, V. N.; Kobayashi, R.; Normand, J.; Raghavachari, K.; Rendell, A.; Burant, J. C.; Iyengar, S. S.; Tomasi, J.; Cossi, M.; Rega, N.; Millam, J. M.; Klene, M.; Knox, J. E.; Cross, J. B.; Bakken, V.; Adamo, C.; Jaramillo, J.; Gomperts, R.; Stratmann, R. E.; Yazyev, O.; Austin, A. J.; Cammi, R.; Pomelli, C.; Ochterski, J. W.; Martin, R. L.; Morokuma, K.; Zakrzewski, V. G.; Voth, G. A.; Salvador, P.; Dannenberg, J. J.; Dapprich, S.; Daniels, A. D.; Farkas, Ö.; Foresman, J. B.; Ortiz, J. V.; Cioslowski, J.; Fox, D. J. *Gaussian 09, Revision B.01*; Gaussian, Inc.: Wallingford, CT, 2009.
(52) Santoro, F.; Lami, A.; Improta, R.; Bloino, J.; Barone, V. Effective Method for The Computation of Optical Spectra of Large Molecules at Finite Temperature Including The Duschinsky and Herzberg−Teller Effect: The Q_x Band of Porphyrin as A Case Study. *J. Chem. Phys.* **2008**, *128*, 224311.
(53) Niu, Y.; Peng, Q.; Deng, C. M.; Gao, X.; Shuai, Z. G. Theory of Excited State Decays and Optical Spectra: Application to Polyatomic Molecules. *J. Phys. Chem. A* **2010**, *114*, 7817−7831.
(54) Kelley, A. M. Resonance Raman and Resonance Hyper-Raman Intensities: Structure and Dynamics of Molecular Excited States in Solution. *J. Phys. Chem. A* **2008**, *112*, 11975−11991.
(55) Radziszewski, J. G.; Gil, M.; Gorski, A.; Spanget-Larsen, J.; Waluk, J.; Mróz, B. J. Electronic States of The Phenoxyl Radical. *J. Chem. Phys.* **2001**, *115*, 9733−9738.
(56) Biczysko, M. ; Bloino, J. ; Santoro, F. ; Barone, V. *Computational Strategies for Spectroscopy. From Small Molecules to Nano Systems*, first ed.; Barone, V., Eds.; Wiley, Ltd.: Chichester, U.K., 2011, pp 300−386.
(57) Santoro, F.; Improta, R.; Lami, A.; Bloino, J.; Barone, V. Effective Method to Compute Franck-Condon Integrals for Optical Spectra of Large Molecules in Solution. *J. Chem. Phys.* **2007**, *126*, 084509.
(58) Du, R.; Liu, C.; Zhao, Y. Y.; Pei, K.-M.; Wang, H.-G.; Zheng, X. M.; Li, M. D.; Xue, J.-D.; Phillips, D. L. Resonance Raman Spectroscopic and Theoretical Investigation of The Excited State Proton Transfer Reaction Dynamics of 2-Thiopyridone. *J. Phys. Chem. B* **2011**, *115*, 8266−8277.
(59) Hehre, W. J. ; Radom, L. ; Schleyer, P. v. R. ; Pople,J. A. *Ab Initio Molecular Orbital Theory*; Wiley: New York, 1996.
(60) Edwards, L.; Dolphin, D. H.; Gouterman, M.; Adler, A. D. Porphyrins XVII. Vapor Absorption Spectra and Redox Reactions: Tetraphenyl-porphins and Porphin. *J. Mol. Spectrosc.* **1971**, *38*, 16.
(61) Minaev, B.; Wang, Y.-H.; Wang, G.-K.; Luo, Y.; Ågren, H. Density Functional Theory Study of Vibronic Structure of The First Absorption Q_x Band in Free-Base Porphin. *Spectrochim. Acta, Part A* **2006**, *65*, 308−323.
(62) Hirata, S.; Head-Gordon, M. Time-Dependent Density Functional Theory within The Tamm-Dancoff Approximation. *Chem. Phys. Lett.* **1999**, *314*, 291−299.